OL | Organic Letters

pubs.acs.org/OrgLett Letter

Switching of C−C and C−N Coupling/Cleavage for Hypersensitive Detection of Cu^{2+} by a Catalytically Mediated 2-Aminoimidazolyl-Tailored Six-Membered Rhodamine Probe

Lin-Lin Yang,[†] A-Ling Tang,[†] Pei-Yi Wang,* and Song Yang*

Cite This: https://dx.doi.org/10.1021/acs.orglett.0c02814 Read Online

ACCESS | Metrics & More | Article Recommendations | Supporting Information

ABSTRACT: A robust six-membered rhodamine spirocyclic probe **1** containing a versatile 2-aminoimidazolyl moiety was elaborately designed and synthesized via an attractive C−C and C−N coupling strategy to improve the performance in the detection of ultralow transition metal ions. Probe **1** allowed the highly hypersensitive detection of Cu^{2+} with a superior picomolar limit of detection (35 pM) and nanomolar naked-eye performance (80 nM) via the switching of C−C and C−N cleavage by a catalytic hydrolysis mode.

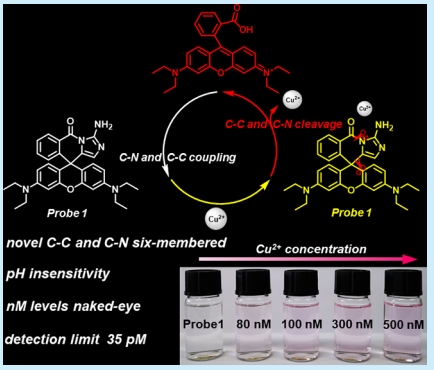

Transition metal ions are naturally indispensable ingredients that are involved in diverse essential physiological and metabolic processes in many living organisms. The loss of their homeostasis is closely associated with diverse dysfunctions and/or hematological manifestations.[1] Copper, one of the critically important transition metals, is responsible for the normal functioning of various organs and metabolic processes.[1a,2] However, Cu^{2+} deficiency can lead to growth failure and neurodegenerative disorders, whereas excessive amounts of Cu^{2+} in biological processes can cause serious syndromes, including Alzheimer's disease,[3] Wilson's disease,[4] and metabolic disorders such as obesity and diabetes.[5] Additionally, superfluous metal ions lead to environmental pollution that seriously threatens the health of plants, microorganisms, and animals, including humans. Thus, monitoring the distribution and dynamic fluctuations of metal ions in subcellular microenvironments and/or ambient surroundings can promote the in-depth understanding of diverse metal-mediated physiological and pathological processes for disease diagnosis and simultaneously track the invisible environmental pollutants for ecological protection.[6]

In the past 50 years, the detection of biologically and/or environmentally important transition metal ions by fluorescent probes, especially a probe for the selective and rapid sensing of Cu^{2+} ions, has experienced explosive development.[7] Since Czarnik et al.[8] reported the pioneering work for the colorimetric detection of Cu^{2+} by using a typical rhodamine-based five-membered spirocyclic hydrazide (**1**) in 1997, a considerable amount of sensitive chromogenic chemosensors for detecting Cu^{2+} ions,[9] in vitro and in cell, have been established by rationally decorating various fluorophores, such as rhodamine,[10] naphthalimide,[11] fluorescein,[12] cyanine dyes,[13] anthracene,[14] and BODIPY.[15] Among these sensors, rhodamine-based fluorescent sensors [such as **1**−**4** (Figure 1)] bearing a classical five-membered spirolactam skeleton have been strongly highlighted and investigated due to their prominent photophysical and photostability properties and can be used to sensitively distinguish Cu^{2+} ions via the flexible regulation of C−N bond cleavage along with fluorescence "turn-on" and/or color transformation.[8,16] Despite the outstanding progress achieved in this field, several challenges and problems persist. These issues include the frequent nanomolar and micromolar levels of the corresponding limit of detection (LOD) and naked-eye recognition for metal ion analytes, and susceptible detection under harsh circumstances. These problems limit the realistic applications of probes for monitoring the dynamic fluctuations of ultralow analytes in subcellular microenvironments and natural environments. For example, the dynamic concentration of free Cu^{2+} ions in mammalian cells is $<10^{-17}$ mol L^{-1},[17] and tap water contains latent nanomolar concentrations of Cu^{2+}. Therefore, developing innovative and practical fluorescent probes for the real-

Received: August 21, 2020

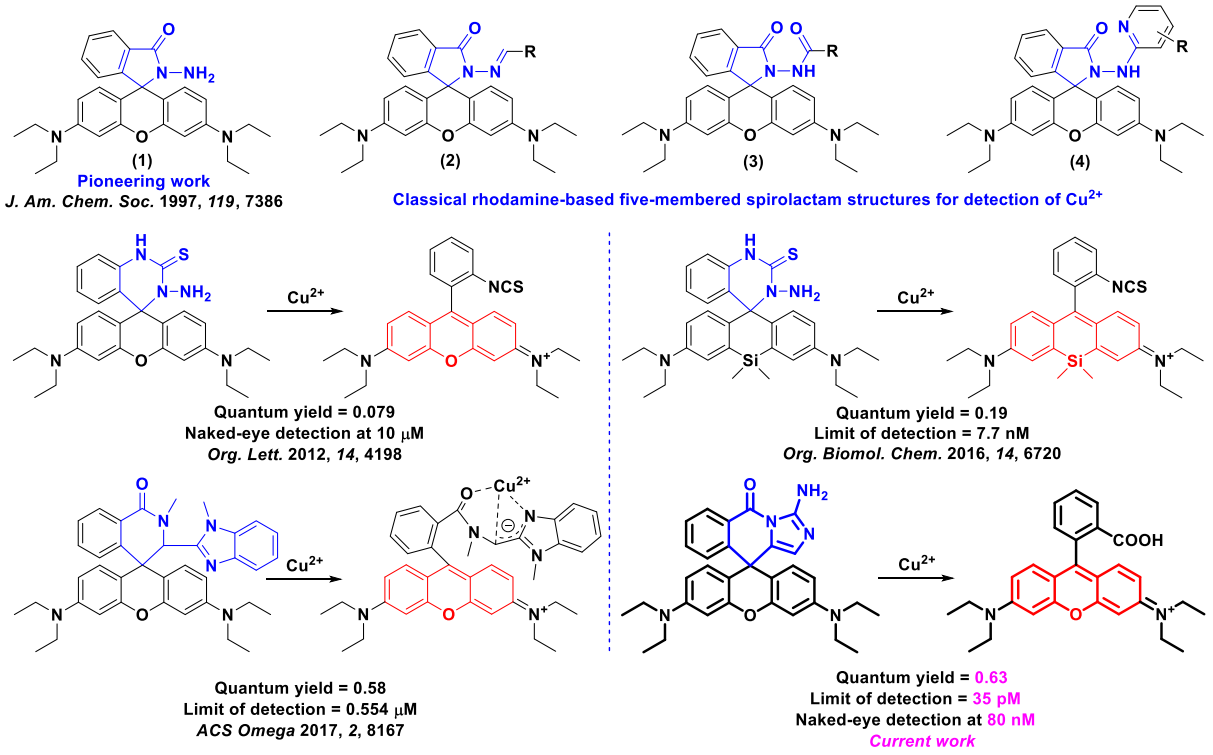

Figure 1. Classical rhodamine-based five-membered spirolactam structures **1**−**4** and six-membered rhodamine spirocyclic probes for the detection of Cu^{2+}.

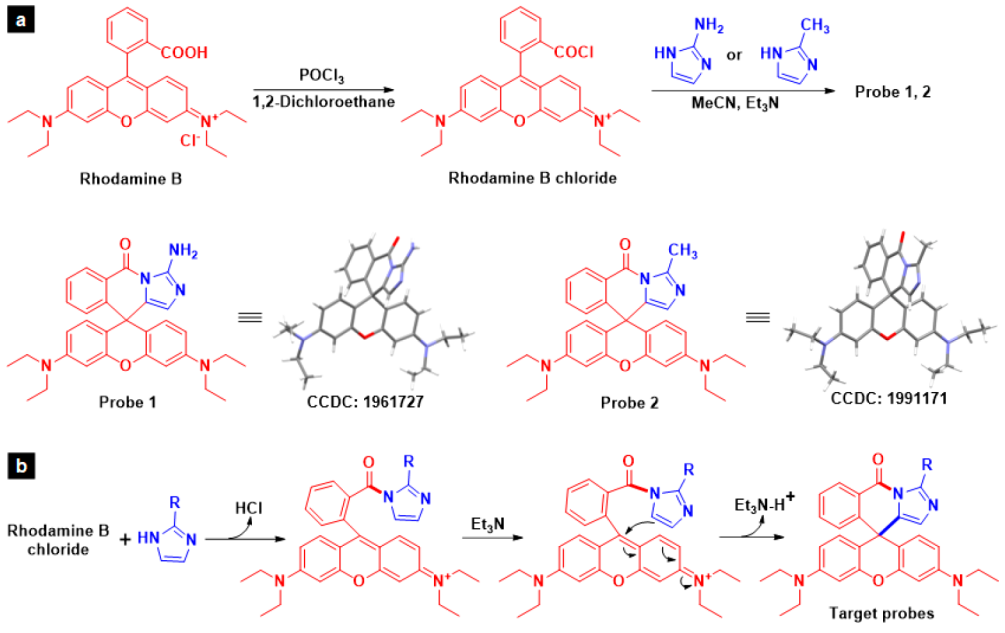

Figure 2. (a) Synthesis of probes **1** and **2**. (b) Proposed mechanism for C−C and C−N coupling six-membered cyclization. R = NH_2 or CH_3.

time, rapid, quantitative, and naked-eye detection of metal ions at nanomolar and picomolar levels is challenging.

Careful investigations have found that traditional rhodamine-based five-membered spirolactam structures can hardly improve the current detection capability for several possible reasons, such as the stereotypical cleavage of C−N bonds, the mode of chelation between analytes and probes, the low efficiency and inadequacy of hydrolysis, and the disturbance of fluorescence caused by nonplanar hydrolysis products.[9,16] Meanwhile, the strained spirolactam structure usually displays an "unstable" characteristic in acidic solutions, thus introducing uncertainty and limitations into its application.[16] Therefore, improving the performance of the classical five-membered spirolactam scaffold and exploring new favorable spirocyclic frameworks are necessary.

Six robust rhodamine-based probes possessing different six-membered spirocyclic skeletons have been recently reported to have perceptible capability for monitoring Cu^{2+},[18] Hg^{2+},[19] and ClO^-.[20] Among them, three probes bearing corresponding six-membered thiosemicarbazide moieties and the spirolactam

https://dx.doi.org/10.1021/acs.orglett.0c02814
Org. Lett. XXXX, XXX, XXX−XXX

pattern (Figure 1) can selectively distinguish Cu^{2+} by involving C−N bond cleavage along with the formation of an isothiocyanate group and the chelation of metal ions along with C−C bond cleavage. Notably, these interesting probes continue to display some limitations, with either a low fluorescence quantum yield[18a,b] or a weak sensitivity.[18c] Inspired by the intriguing frameworks mentioned above, the rational fabrication of innovative six-membered spirocycles may advance the performance and provide highly reliable and hypersensitive fluorescent chemosensors for the detection of metal ions at ultralow concentrations. For this purpose, herein, a robust six-membered rhodamine spirocyclic probe **1** containing a versatile 2-aminoimidazolyl moiety was elaborately designed and synthesized on the basis of an attractive C−C and C−N coupling structure. This probe is reported for the first time and confirmed on the basis of its single-crystal structure, which is distinctly different from classical five-membered spirolactam structures. Within this molecule, the versatile 2-amino-carbonyl imidazole motif executes a dual function: promoting the binding affinity[21] for Cu^{2+} to induce the rearrangement of the whole molecular electronic property accompanied by subsequent C−C bond cleavage and accelerating the Cu^{2+}-mediated catalytic hydrolysis[22] of carbonyl imidazole along with C−N bond cleavage. On the basis of this proposal, we expect that this probe can achieve ultralow Cu^{2+} detection by elaborately exploiting the compelling C−C and C−N cleavage approach along with the release of violently fluorescent and colorimetric rhodamine. Probe **1** displayed highly selective and hypersensitive detection of Cu^{2+} with a superior picomolar LOD and nanomolar naked-eye performance.

A facile synthetic route for the construction of rhodamine-based C−N- and C−C coupling six-membered fluorescent probes **1** and **2** is illustrated in Figure 2a. Generally, rhodamine B was treated with $POCl_3$ to provide a chlorinated intermediate, which was then reacted with 2-aminoimidazole or 2-methylimidazole under the mediation of the base triethylamine to afford final product **1** or **2**, respectively. A possible mechanism for the C−N and C−C coupling six-membered cyclization was proposed as shown in Figure 2b. The frameworks of probes **1** and **2** were confirmed on the basis of NMR and HRMS analyses and their relevant single-crystal structures (Figures S1−S8 and Tables S1 and S2).

The fluorescence responses of probe **1** before and after the addition of Cu^{2+} ions in various organic solvents or water/organic solvents were investigated to acquire an improved system for Cu^{2+} ion detection. Notably, excellent detection performance was obtained in an acetonitrile solvent with 770-fold fluorescence enhancement after incubation with an equivalent amount of Cu^{2+} for 10 min at 25 °C (Figure S9). Subsequently, an acetonitrile/water mixed solution [3:7 (v/v)] was applied in the following tests (Figure S10). Further spectroscopy investigations were executed to evaluate the selectivity and sensitivity of probe **1**. As depicted in Figure 3a−c, violet fluorescence at 578 nm (Φ = 0.63) and strong absorption at 556 nm along with a naked-eye recognition effect were triggered and generated only after the addition of Cu^{2+} but not that of other metal ions, indicating that a reliable colorimetric probe for detecting Cu^{2+} was established. Competition experiments revealed the anti-interference performance of probe **1** for distinguishing Cu^{2+}, leading to the fluorescence "turn on" only by the latter supplementation of Cu^{2+} (Figures S11 and S12). A titration experiment on

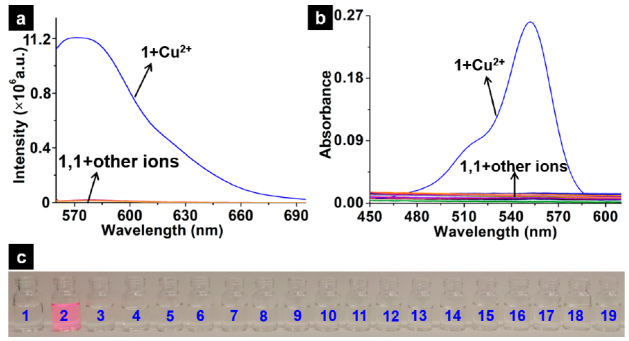

Figure 3. (a) Fluorescence and (b) absorption spectra of probe **1** (10 μM) upon addition of 10 μM Cu^{2+} and other ions [λ_{ex} = 556 nm, slits 3/3, 3:7 (v/v) CH_3CN/H_2O]. (c) Probe **1** (10 μM) upon addition of 10 μM metal ions: (1) probe **1**, (2) Cu^{2+}, (3) Ca^{2+}, (4) Ni^{2+}, (5) Ba^{2+}, (6) Cr^{3+}, (7) Co^{2+}, (8) Hg^{2+}, (9) Al^{3+}, (10) Fe^{3+}, (11) Zn^{2+}, (12) Li^{+}, (13) Pb^{2+}, (14) Cd^{2+}, (15) Mg^{2+}, (16) K^{+}, (17) Na^{+}, (18) Ag^{+}, and (19) Fe^{2+}.

probe **1** toward various dosages of Cu^{2+} revealed a predominant linear detection range of 30−1300 nM [R^2 = 0.9924 (Figure S13)], suggesting that this probe could enable the quantitative analysis of Cu^{2+} at the nanomolar level. A superior picomolar LOD (35 pM, 2.22 ppt) and nanomolar naked-eye performance [80 nM, 5.08 ppb (Figure S14)] were achieved, further confirming that probe **1** could serve as an extremely superior tool for selective and hypersensitive detection of Cu^{2+}, thus demonstrating that the rational design of the six-membered rhodamine spirocyclic probe could improve the performance of classical five-membered spirolactam structures in the detection of metal ions. Additionally, this probe showed a particularly robust performance in detecting Cu^{2+} over a harsh pH range of 3.6−11.6 in CH_3CN/HEPES buffer (Figure S15). By contrast, probe **2** showed insignificant detection effects toward Cu^{2+} (Figure S16), indicating that the amino part promoted the binding affinity[21] with Cu^{2+} to induce the rearrangement of the whole molecular electronic property accompanied by subsequent C−C bond cleavage.

The time-dependent fluorescence intensity of probe **1** triggered by diverse Cu^{2+} concentrations was recorded to investigate the detection mechanism of the probe. At Cu^{2+} concentrations of 10, 7.5, 5, and 2.5 μM, the final fluorescence intensity could reach a stable equilibrium at approximately 5, 9, 15, and 45 min, respectively, indicating a catalytic mode for detecting Cu^{2+} (Figure 4a). A distinct blue shift from 587 to 578 nm was observed as illustrated in Figure 4b. This shift might be ascribed to the transformation of the C−C severed product into C−C and C−N severed products (Figure 5). After the purification and identification of the final fluorescent product, the original rhodamine returned (Figures S17−S19), validating our initial assumption. Meanwhile, a ^1H NMR titration experiment (Figure S20) was performed to reveal the detection mechanism. Multiple newly generated small peaks were observed after the introduction of Cu^{2+}, indicating that a complicated component was probably created by either C−C cleavage or both C−C and C−N cleavage. High-performance liquid chromatography (HPLC) of probe **1** reacting with Cu^{2+} was provided to monitor the process of catalytic hydrolysis. As shown in Figures S21−S39, Cu^{2+} detection was definitely directed by a catalytic hydrolysis mode and affording a final conversion yield to rhodamine with 95.4%, in agreement with our original design.

https://dx.doi.org/10.1021/acs.orglett.0c02814
Org. Lett. XXXX, XXX, XXX−XXX

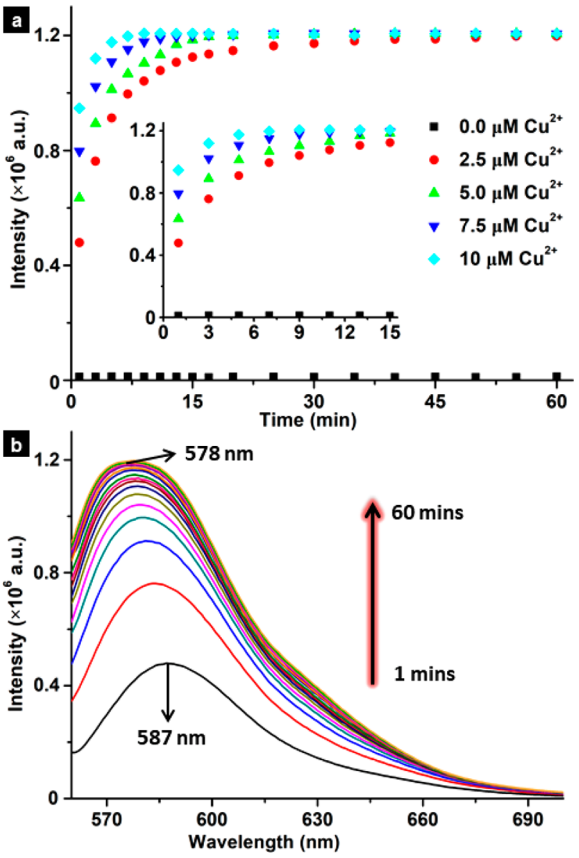

Figure 4. Time-dependent fluorescence intensity spectra of (a) probe **1** (10 μM) reacted with various concentrations of Cu^{2+} and (b) probe 1 (10 μM) upon the detection of 2.5 μM Cu^{2+}. λ_{ex} = 556 nm, slits 3/3, CH_3CN:H_2O = 3:7.

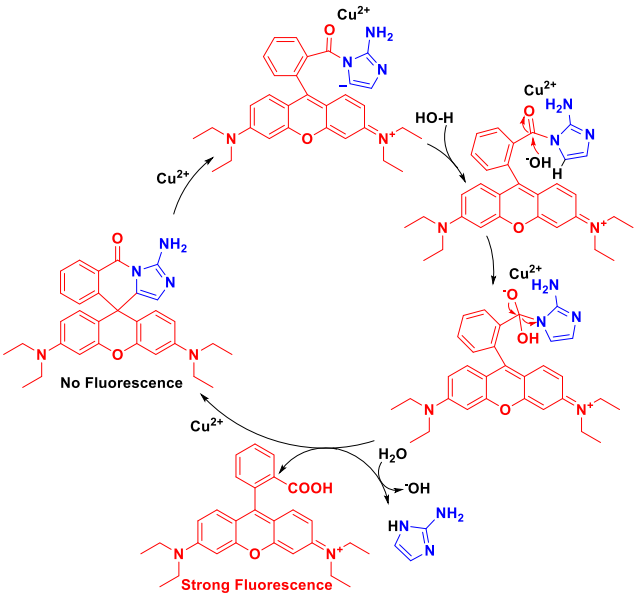

Figure 5. Possible mechanism for Cu^{2+}-induced catalytic hydrolysis sensing cycle of probe **1** in a CH_3CN/H_2O solution.

A549 cells were used for fluorescence imaging to explore the cell detection capability of probe **1** toward Cu^{2+}. Initially, probe **1** showed low cytotoxicity toward mammalian cell lines measured via MTT assays (Figure S40). Briefly, A549 cells were incubated with 5 μM probe **1** for 0.5 h at 37 °C, washed with PBS buffer (0.01 M, pH 7.4) thrice, and subsequently treated with 5 μM Cu^{2+} for 1 h at 37 °C. Finally, the cells were washed with PBS buffer thrice before being imaged. Cells with strong red fluorescence (Figure 6) were observed only by

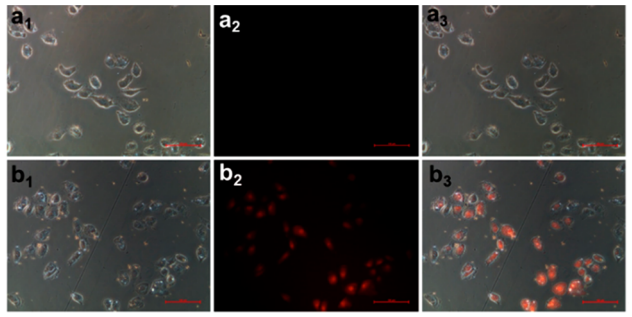

Figure 6. Fluorescence imaging of probe **1** responding to Cu^{2+} in living A549 cells. (a_1) Bright-field and (a_2) fluorescence images of A549 cells incubated with 5 μM probe **1** for 30 min at 37 °C. (a_3) Merged image of panels a_1 and a_2. (b_1) Bright-field and (b_2) fluorescence images of A549 cells incubated with 5 μM probe **1** and then 5 μM Cu^{2+} for 1 h at 37 °C. (b_3) Merged image of panels b_1 and b_2. Red channel, 510−560 nm.

incubating the cells with probe **1** upon addition of Cu^{2+}, thereby indicating that probe **1** could penetrate the cell membrane and selectively detect Cu^{2+} in cell.

In summary, a robust six-membered rhodamine spirocyclic probe **1** containing a versatile 2-aminoimidazolyl moiety was rationally designed and constructed via an attractive C−C and C−N coupling strategy to improve the performance encountered by classical five-membered spirolactam structures in ultralow metal ion detection. The results of testing found that probe **1** displayed highly selective and hypersensitive detection of Cu^{2+} with an excellent picomolar LOD (35 pM, 2.22 ppt) and nanomolar naked-eye performance (80 nM, 5.08 ppb) via a catalytically mediated C−C and C−N cleavage along with violent fluorescence "turn-on" (Φ = 0.63, for the new product). A significant linear detection range of 30−1300 nM was afforded for the quantification of nanomolar levels of Cu^{2+}. Further bioimaging studies revealed that probe **1** showed good cell membrane permeability and practicable capability for monitoring Cu^{2+} in living cell lines. We anticipate that this intriguing C−C and C−N coupling/cleavage approach can open up a new avenue for developing hypersensitive fluorescent probes for the desired ultralow analyte detection, which improves our understanding of diverse metal-mediated physiological and pathological processes for disease diagnosis.

■ ASSOCIATED CONTENT

Supporting Information

The Supporting Information is available free of charge at https://pubs.acs.org/doi/10.1021/acs.orglett.0c02814.

Materials and methods; synthesis, NMR, HRMS, and crystal structures of probes **1** and **2**; calculation of the relative fluorescence quantum yields and detection limit; sensitivity of probe **1** for Cu^{2+} in different solvents; competition experiments; quantitative determination of Cu^{2+}; detection of nanomolar level Cu^{2+} by the naked eye; influence of pH on the detection of Cu^{2+}; sensitivity of probe **2** toward Cu^{2+}; ^1H NMR and HRMS spectra for the newly generated product; HPLC analysis of

https://dx.doi.org/10.1021/acs.orglett.0c02814
Org. Lett. XXXX, XXX, XXX−XXX

probe **1** reacting with Cu^{2+}; imaging experiments using the chelating agent of Cu^{2+}; and a comparison of detection results of reported five- and six-membered rhodamine-based probes (PDF)

Accession Codes

CCDC 1961727 and 1991171 contain the supplementary crystallographic data for this paper. These data can be obtained free of charge via www.ccdc.cam.ac.uk/data_request/cif, or by emailing data_request@ccdc.cam.ac.uk, or by contacting The Cambridge Crystallographic Data Centre, 12 Union Road, Cambridge CB2 1EZ, UK; fax: +44 1223 336033.

AUTHOR INFORMATION

Corresponding Authors

Song Yang − *State Key Laboratory Breeding Base of Green Pesticide and Agricultural Bioengineering, Key Laboratory of Green Pesticide and Agricultural Bioengineering, Ministry of Education, Guizhou University, Guiyang 550025, China;* orcid.org/0000-0003-1301-3030; Email: jhzx.msm@gmail.com

Pei-Yi Wang − *State Key Laboratory Breeding Base of Green Pesticide and Agricultural Bioengineering, Key Laboratory of Green Pesticide and Agricultural Bioengineering, Ministry of Education, Guizhou University, Guiyang 550025, China;* orcid.org/0000-0002-9904-0664; Email: pywang888@126.com

Authors

Lin-Lin Yang − *State Key Laboratory Breeding Base of Green Pesticide and Agricultural Bioengineering, Key Laboratory of Green Pesticide and Agricultural Bioengineering, Ministry of Education, Guizhou University, Guiyang 550025, China*

A-Ling Tang − *State Key Laboratory Breeding Base of Green Pesticide and Agricultural Bioengineering, Key Laboratory of Green Pesticide and Agricultural Bioengineering, Ministry of Education, Guizhou University, Guiyang 550025, China*

Complete contact information is available at: https://pubs.acs.org/10.1021/acs.orglett.0c02814

Author Contributions

†L.-L.Y. and A-L.T. contributed equally to this work.

Notes

The authors declare no competing financial interest.

ACKNOWLEDGMENTS

The authors acknowledge the financial support of the National Natural Science Foundation of China (21702037, 21662009, 31860516, and 21877021), the Research Project of the Ministry of Education of China (20135201110005 and 213033A), the Key Technologies R&D Program (2014BAD23B01), the Guizhou Provincial S&T Program ([2017]5788), and the Program of Introducing Talents of Discipline to Universities of China (111 Program, D20023).

REFERENCES

(1) (a) Carter, K. P.; Young, A. M.; Palmer, A. E. *Chem. Rev.* **2014**, *114*, 4564−4601. (b) Barnham, K. J.; Bush, A. I. *Chem. Soc. Rev.* **2014**, *43*, 6727−6749.

(2) Gaggelli, E.; Kozlowski, H.; Valensin, D.; Valensin, G. *Chem. Rev.* **2006**, *106*, 1995−2044.

(3) (a) Barnham, K. J.; Masters, C. L.; Bush, A. I. *Nat. Rev. Drug Discovery* **2004**, *3*, 205−214. (b) Savelieff, M. G.; Lee, S.; Liu, Y.; Lim, M. H. *ACS Chem. Biol.* **2013**, *8*, 856−865. (c) Multhaup, G.; Schlicksupp, A.; Hesse, L.; Beher, D.; Ruppert, T.; Masters, C. L.; Beyreuther, K. *Science* **1996**, *271*, 1406−1409. (d) Lee, S.; Barin, G.; Ackerman, C. M.; Muchenditsi, A.; Xu, J.; Reimer, J. A.; Lutsenko, S.; Long, J. R.; Chang, C. J. *J. Am. Chem. Soc.* **2016**, *138*, 7603−7609.

(4) (a) Lutsenko, S. *Biochem. Soc. Trans.* **2008**, *36*, 1233−1238. (b) Huster, D. *Ann. N. Y. Acad. Sci.* **2014**, *1315*, 37−44.

(5) (a) Huster, D.; Purnat, T. D.; Burkhead, J. L.; Ralle, M.; Fiehn, O.; Stuckert, F.; Olson, N. E.; Teupser, D.; Lutsenko, S. *J. Biol. Chem.* **2007**, *282*, 8343−8355. (b) Huster, D.; Lutsenko, S. *Mol. BioSyst.* **2007**, *3*, 816−824. (c) Engle, T. E. *J. Anim. Sci.* **2011**, *89*, 591−596.

(6) (a) Zhu, H.; Fan, J.; Wang, B.; Peng, X. *Chem. Soc. Rev.* **2015**, *44*, 4337−4366. (b) Cao, D.; Liu, Z.; Verwilst, P.; Koo, S.; Jangjili, P.; Kim, J. S.; Lin, W. *Chem. Rev.* **2019**, *119*, 10403−10519.

(7) Wu, D.; Sedgwick, A. C.; Gunnlaugsson, T.; Akkaya, E. U.; Yoon, J.; James, T. D. *Chem. Soc. Rev.* **2017**, *46*, 7105−7123.

(8) For pioneering five-membered works, see: Dujols, V.; Ford, F.; Czarnik, A. W. *J. Am. Chem. Soc.* **1997**, *119*, 7386−7387.

(9) Sivaraman, G.; Iniya, M.; Anand, T.; Kotla, N. G.; Sunnapu, O.; Singaravadivel, S.; Gulyani, A.; Chellappa, D. *Coord. Chem. Rev.* **2018**, *357*, 50−104.

(10) (a) Kumar, M.; Kumar, N.; Bhalla, V.; Sharma, P. R.; Kaur, T. *Org. Lett.* **2012**, *14*, 406−409. (b) Liu, C.; Jiao, X.; Wang, Q.; Huang, K.; He, S.; Zhao, L.; Zeng, X. *Chem. Commun.* **2017**, *53*, 10727−10730. (c) Huo, F.; Wang, L.; Yin, C.; Yang, Y.; Tong, H.; Chao, J.; Zhang, Y. *Sens. Actuators, B* **2013**, *188*, 735−740. (d) Wang, L.; Du, W.; Hu, Z.; Uvdal, K.; Li, L.; Huang, W. *Angew. Chem., Int. Ed.* **2019**, *58*, 14026−14043. (e) Zhou, L.; Zhang, X.; Wang, Q.; Lv, Y.; Mao, G.; Luo, A.; Wu, Y.; Wu, Y.; Zhang, J.; Tan, W. *J. Am. Chem. Soc.* **2014**, *136*, 9838−9841. (f) Liu, Y.; Su, Q.; Chen, M.; Dong, Y.; Shi, Y.; Feng, W.; Wu, Z. Y.; Li, F. *Adv. Mater.* **2016**, *28*, 6625−6630.

(11) (a) Goswami, S.; Sen, D.; Das, N. K. *Org. Lett.* **2010**, *12*, 856−859. (b) Li, M.; Ge, H.; Arrowsmith, R. L.; Mirabello, V.; Botchway, S. W.; Zhu, W.; Pascu, S. I.; James, T. D. *Chem. Commun.* **2014**, *50*, 11806−11809.

(12) (a) Yang, Y.; Huo, F.; Yin, C.; Chu, Y.; Chao, J.; Zhang, Y.; Zhang, J.; Li, S.; Lv, H.; Zheng, A.; Liu, D. *Sens. Actuators, B* **2013**, *177*, 1189−1197. (b) Choi, M. G.; Cha, S.; Lee, H.; Jeon, H. L.; Chang, S. K. *Chem. Commun.* **2009**, 7390−7392. (c) Huo, F. J.; Yin, C. X.; Yang, Y. T.; Su, J.; Chao, J. B.; Liu, D. S. *Anal. Chem.* **2012**, *84*, 2219−2223.

(13) (a) Li, P.; Duan, X.; Chen, Z.; Liu, Y.; Xie, T.; Fang, L.; Li, X.; Yin, M.; Tang, B. *Chem. Commun.* **2011**, *47*, 7755−7757. (b) Hirayama, T.; Van de Bittner, G. C.; Gray, L. W.; Lutsenko, S.; Chang, C. J. *Proc. Natl. Acad. Sci. U. S. A.* **2012**, *109*, 2228−2233.

(14) (a) Xie, Y.; Ding, Y.; Li, X.; Wang, C.; Hill, J. P.; Ariga, K.; Zhang, W.; Zhu, W. *Chem. Commun.* **2012**, *48*, 11513−11515. (b) Yang, L.; Song, Q.; Damit-Og, K.; Cao, H. *Sens. Actuators, B* **2013**, *176*, 181−185.

(15) Li, Q.; Guo, Y.; Shao, S. *Sens. Actuators, B* **2012**, *171*, 872−877.

(16) Chen, X.; Pradhan, T.; Wang, F.; Kim, J. S.; Yoon, J. *Chem. Rev.* **2012**, *112*, 1910−1956.

(17) Rae, T. D.; Schmidt, P. J.; Pufahl, R. A.; Culotta, V. C.; O'Halloran, T. V. *Science* **1999**, *284*, 805−808.

(18) (a) Wu, C.; Bian, Q. N.; Zhang, B. G.; Cai, X.; Zhang, S. D.; Zheng, H.; Yang, S. Y.; Jiang, Y. B. *Org. Lett.* **2012**, *14*, 4198−4201. (b) Wang, B.; Cui, X.; Zhang, Z.; Chai, X.; Ding, H.; Wu, Q.; Guo, Z.; Wang, T. *Org. Biomol. Chem.* **2016**, *14*, 6720−6728. (c) Majumdar, A.; Lim, C. S.; Kim, H. M.; Ghosh, K. *ACS Omega* **2017**, *2*, 8167−8176.

(19) (a) Yang, Z.; Hao, L.; Yin, B.; She, M.; Obst, M.; Kappler, A.; Li, J. *Org. Lett.* **2013**, *15*, 4334−4337. (b) Biswal, B.; Mallick, D.; Bag, B. *Org. Biomol. Chem.* **2016**, *14*, 2241−2248.

(20) Wang, Z.; Zhang, Q.; Liu, J.; Sui, R.; Li, Y.; Li, Y.; Zhang, X.; Yu, H.; Jing, K.; Zhang, M.; Xiao, Y. *Anal. Chim. Acta* **2019**, *1082*, 116−125.

(21) Xie, P.; Guo, F.; Li, D.; Liu, X.; Liu, L. *J. Lumin.* **2011**, *131*, 104−108.
(22) (a) Yang, Y.; Zhao, Q.; Feng, W.; Li, F. *Chem. Rev.* **2013**, *113*, 192−270. (b) Kroll, H. *J. Am. Chem. Soc.* **1952**, *74*, 2036−2039. (c) Bender, M. L.; Turnquest, B. W. *J. Am. Chem. Soc.* **1957**, *79*, 1889−1893.

https://dx.doi.org/10.1021/acs.orglett.0c02814
Org. Lett. XXXX, XXX, XXX−XXX